Thermodynamic Parameters To Predict Stability of RNA/DNA Hybrid Duplexes†

Naoki Sugimoto,* Shu-ichi Nakano, Misa Katoh, Akiko Matsumura, Hiroyuki Nakamuta, Tatsuo Ohmichi, Mari Yoneyama, and Muneo Sasaki

Department of Chemistry, Faculty of Science, Konan University, 8-9-1 Okamoto, Higashinada-ku, Kobe 658, Japan

Received April 21, 1995; Revised Manuscript Received June 12, 1995®

ABSTRACT: The thermodynamic parameters ($\Delta H°$, $\Delta S°$, and $\Delta G°_{37}$) for 16 nearest-neighbor sets and one initiation factor are presented here in order to predict stability of RNA/DNA hybrid duplexes. To determine the nearest-neighbor parameters, thermodynamics for 68 different hybrid sequences (136 single-stranded oligonucleotides) with 5−13 nucleotide length including several duplexes with identical nearest-neighbors were measured by UV melting procedure. These sequences were selected to have many different combinations of nearest-neighbor pairs, and so that the number of the 16 nearest-neighbor sequences in the oligomers were as equal as possible. The structures of the hybrids were also investigated by measuring circular dichroism spectra. Comparing $\Delta G°_{37}$ values of the hybrids with DNA/DNA and RNA/RNA parameters reported previously (Breslauer, K. J., Frank, R., Blöcker, H., & Marky, L. A. (1986) *Proc. Natl. Acad. Sci. U.S.A. 83,* 3746−3750; Freier, S. M., Kierzek, R., Jaeger, J. A., Sugimoto, N., Caruthers, M. H., Neilson, T., & Turner, D. H. (1986) *Proc. Natl. Acad. Sci. U.S.A. 83,* 9373−9377), RNA/RNA double helix is the most stable of the three kinds of helixes with the same nearest-neighbor sequences. Which is more stable between DNA/DNA and RNA/DNA hybrid duplexes depends on its sequence. Calculated thermodynamic values of hybrid formation with the present parameters reproduce the experimental values within reasonable errors.

In biological systems, RNA/DNA double helixes (hybrids) occur in Okazaki fragments (Ogawa & Okazaki, 1980), during RNA transcription (Yager & von Hippel, 1991), during reverse transcription of retroviruses (Varmus, 1982), and in antisense therapy (Stein & Cheng, 1993; Shimayama et al., 1993). For rational optimization of these approaches, it is necessary to know quantitatively the hybrid stability. However, little is known about the thermodynamics of RNA/DNA hybrid formation and the parameters for predicting its stability.

Thermodynamic parameters based on the nearest-neighbor model were determined for stabilities of DNA/DNA and RNA/RNA duplexes (Breslauer et al., 1986; Freier et al., 1986), and they were applied to predict stable secondary structures and active centers of nucleic acids (Sugimoto et al., 1991, 1993; LeCuyer et al., 1993; Connell & Yarus, 1994). Thermodynamic parameters were also reported for formation of mismatches, dangling ends, internal loops, bulges, and hairpin loops in RNA (Sugimoto et al., 1986, 1987a,b; Turner et al., 1990; Longfellow et al., 1990; Peritz et al., 1991). It is not reasonable to apply these parameters to the prediction of hybrid formation because the characteristics of hybrids are different from those of DNA/DNA and RNA/RNA duplexes. Thus, it is necessary to obtain new thermodynamic parameters to predict the stability of RNA/DNA hybrid formation.

Here, in order to determine the nearest-neighbor parameters to predict hybrid stability, thermodynamics for 68 different hybrid sequences (136 single-stranded oligonucleotides) with 5−13 nucleotide length including several duplexes with identical nearest neighbors were investigated by UV[1] melting procedure. Then, the thermodynamic parameters ($\Delta H°$, $\Delta S°$, and $\Delta G°_{37}$) for 16 nearest-neighbor sets and one initiation factor are obtained. The structures of typical hybrids were also investigated by circular dichroism spectroscopy. Comparing calculated thermodynamic values of hybrid formation by using the present parameters with the experimental results, the parameters can reproduce the experimental values within reasonable error.

MATERIALS AND METHODS

Materials. Sixty-eight oligoribonucleotides and 68 oligodeoxyribonucleotides were synthesized chemically on a solid support using phosphoramidite procedures and purified with HPLC after deblocking operations (Kierzek et al., 1986). These 136 oligomers were further purified and desalted with a C-18 Sep-Pak cartridge column. Final purity of the oligomers was confirmed to be greater than at least 98% by HPLC.

These oligonucleotides consist of 16 nearest-neighbor sequences of the Watson−Crick base pairs. The sequences were selected to have many different combinations of nearest-neighbor pairs. The length of the examined hybrid strands was at least 5 nucleotides consisting of four nearest-neighbor pairs and one initiation factor, and at most 13-nucleotides length possessing 12 nearest-neighbor pairs and an initiation factor. All sequences used here comprise several nearest-neighbor pairs and the initiation factor.

All experiments were conducted in a buffer which was 1 M NaCl/10 mM Na_2HPO_4/1 mM Na_2EDTA, pH 7.0. Single-

† This work was supported in part by grants from the Ministry of Education, Science and Culture, Japan, and Hirao Science Foundation to N.S.

* To whom correspondence should be addressed.

® Abstract published in *Advance ACS Abstracts,* August 1, 1995.

[1] Abbreviations: UV, ultraviolet; CD, circular dichroism; HPLC, high-performance liquid chromatography; T_m, melting temperature; Na_2-EDTA, disodium ethylenediaminetetraacetate.

0006-2960/95/0434-11211$09.00/0

strand concentrations of the oligonucleotides were determined by measuring the absorbance at 260 or 280 nm at a high temperature as described previously (Sugimoto et al., 1986). Single-strand extinction coefficients were calculated from mononucleotide and dinucleotide data by using a nearest-neighbor approximation (Richards, 1975). RNA strand and its complementary DNA strand were mixed with a 1:1 concentration ratio to obtain each RNA/DNA hybrid.

CD Measurements. CD spectra were obtained on a JASCO J-600 spectropolarimeter equipped with the temperature controller and interfaced to a NEC PC-9801 computer. The experimental temperature was 5.0 °C. The cuvette-holding chamber was flushed with a constant stream of dry N_2 gas to avoid water condensation on the cuvette exterior. All CD spectra were measured from 350 to 200 nm in 0.1 cm path length cuvettes. The concentration of the samples was 70 μM in 1 M NaCl−phosphate buffer.

UV Measurements. Absorbance measurements in the UV region were made on Hitachi U-3200 and U-3210 spectrophotometers. Melting curves (absorbance vs temperature curves) were measured at 260 nm with these spectrophotometers connected to Hitachi SPR-7 and SPR-10 thermoprogrammers. The heating rate was 0.5 or 1.0 °C/min. The water condensation on the cuvette exterior at the low temperature range was avoided by flushing with a constant stream of dry N_2 gas.

The melting curves of all the hybrids showed normal melting behaviors as DNA/DNA and RNA/RNA double helixes did. Melting data were collected and fitted with NEC PC-9801 computers. The melting temperatures (T_m) were obtained with the curve fitting procedure described previously (Petersheim & Turner, 1983; Sugimoto et al., 1991). The thermodynamic parameters ($\Delta H°$, $\Delta S°$, and $\Delta G°_{37}$) for each hybrid formation were determined as the average values obtained by the following two methods (Petersheim & Turner, 1983; Sugimoto et al., 1986): (I) enthalpy and entropy changes derived from fitting individual melting curves to a two-state model with sloping base lines were averaged, and (II) reciprocal melting temperature T_m^{-1} was plotted vs $\ln(C_t)$ to give enthalpy and entropy changes as described in detail in the Results.

Calculation of Nearest-Neighbor Parameters. According to a nearest-neighbor model, a free energy change ($\Delta G°_{37}$) of the non-self-complementary double-helix formation consists of two terms: (I) a free energy change for helix initiation to form a first base pair in the double helix and (II) a free energy change for helix propagation which is a sum of each subsequent base pair. In a free energy change for helix propagation, there are 16 nearest-neighbor sequences for RNA/DNA hybrids, while there are only ten nearest-neighbor pairs for RNA/RNA or DNA/DNA double helices (Breslauer et al., 1986; Freier et al., 1986). Thus, the parameters of 16 nearest-neighbor sequences and one initiation factor were determined with a nonlinear least-squares computer program (McCalla, 1967; Bevington, 1969). Each nearest-neighbor parameter of $\Delta G°_{37}$ and $\Delta H°$ was decided on the program by 0.1 kcal mol^{-1} step so as to predict the stabilities of all hybrids appling to a two-state model with minimum sum of squares-error values. Then the values of $\Delta S°$ were estimated by the determined values of $\Delta G°_{37}$ and $\Delta H°$. Predicted melting temperatures at 100 μM strand concentration were also calculated.

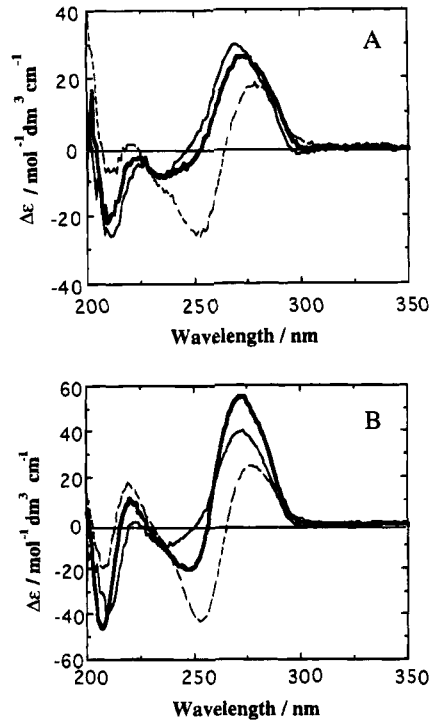

FIGURE 1: CD spectra of (A) r(GCCGUGAG)/r(CUCACGGC) (—), d(GCCGTGAG)/d(CTCACGGC) (- - -), and r(GCCGUGAG)/d(CTCACGGC) (bold —), and (B) r(CUUACGCU)/r(AGCGUAAG) (—), d(CTTACGCT)/d(AGCGTAAG) (- - -), and r(CUUACGCU)/d(AGCGTAAG) (bold —). Each oligomer concentration was 70 μM, and measurements were done in 1 M NaCl−phosphate buffer at 5.0 °C.

RESULTS

Structure of RNA/DNA Hybrid Duplexes. It is known that a CD spectrum of a DNA/DNA double helix has a positive peak around 280 nm and an intense negative peak around 250 nm, consistent with B-form conformation (Ivanov et al., 1973). On the other hand, a spectrum of an RNA/RNA double helix has a positive peak around 270 nm and a relatively weak and negative peak around 235 nm, indicating a normal A-form structure (Hall & McLaughlin, 1991; Ratmeyer et al., 1994).

Figure 1A shows CD spectra of d(GCCGTGAG)/d(CTCACGGC), r(GCCGUGAG)/r(CUCACGGC), and r(GCCGUGAG)/d(CTCACGGC) double helixes at 5.0 °C. In the case of the RNA/DNA hybrid, the spectrum in Figure 1A possesses an intense positive peak around 275 nm and a small negative peak around 230 nm. The spectrum of the RNA/DNA hybrid is between those of the DNA/DNA and the RNA/RNA double helixes, though it resembles relatively more that of the RNA/RNA double helix. By contrast, it was reported that a CD spectrum of $r(CUUC)_3/d(GAAG)_3$ hybrid was relatively similar to that of $d(CTTC)_3/d(GAAG)_3$ (DNA/DNA) duplex (Ratmeyer et al., 1994). Figure 1B shows CD spectra of d(CTTACGCT)/d(AGCGTAAG), r(CUUACGCU)/r(AGCGUAAG), and r(CUUACGCU)/d(AGCGTAAG) double helixes at 5.0 °C. The CD spectrum of the RNA/DNA hybrid has the large positive peak around 275 nm which is larger than not only the peak of the DNA/DNA but the peak of the RNA/RNA. These results suggest that CD spectra of hybrids sometimes look like that of RNA/RNA or DNA/DNA, and sometimes not.

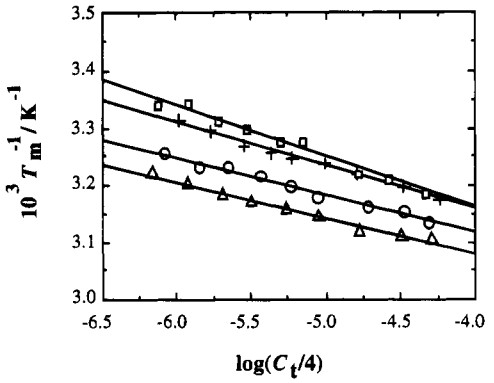

FIGURE 2: T_m^{-1} vs ln(C_t/4) plots of r(UGCUGUUG)/d(CAACAGCA) (□), r(UUACAGCG)/d(CGCTGTAA) (+), r(CGCUGUUAG)/d(CTAACAGCG) (○), and r(CUAACAGCG)/d(CGCTGTTAG) (△). Measurements were done in 1 M NaCl−phosphate buffer at different oligomer concentrations.

Melting Behaviors for RNA/DNA Hybrids. The following equation (Turner et al., 1990) can be applied to melting analysis:

$$T_m^{-1} = [R \ln(C_t/n) + \Delta S^\circ]/\Delta H^\circ \quad (1)$$

where T_m is the melting temperature of a double helix, ΔH° and ΔS° are calculated enthalpy and entropy changes for duplex formation, respectively, R is the gas constant, C_t is the total strand concentration, and n reflects the symmetry factor, which is 1 in the case of self-complementary strands and 4 in the case of non-self-complementary strands. Here, as we need not consider the self-complementary strands, n = 4. Figure 2 shows typical T_m^{-1} vs ln(C_t/4) plots of the RNA/DNA hybrid duplexes measured here, such as r(UGCUGUUG)/d(CAACAGCA), r(UUACAGCG)/d(CGCTGTAA), r(CGCUGUUAG)/d(CTAACAGCG), and r(CUAACAGCG)/d(CGCTGTTAG). In Figure 2, the melting temperatures decrease with decreasing total strand concentrations, and the T_m^{-1} vs ln(C_t/4) plots are linear. The plots gave us the thermodynamic parameters (ΔH°, ΔS°, and ΔG°_{37}) for hybrid formation. Whether these hybrids were two-state transitions is determined with the comparison of the thermodynamics between the T_m^{-1} vs ln(C_t/4) plot and the curve fitting procedure. The thermodynamic parameters obtained with the T_m^{-1} vs ln(C_t/4) plot and the curve fitting procedure are given in the supporting information. When the difference between these thermodynamic values was within 10%, the melting behavior of the hybrid duplex was regarded as a two-state transition. Consequently, only four hybrids, r(CGUGC)/d(GCACG), r(GCACG)/d(CGTGC), r(UUUGUAUCCAAU)/d(ATTGGATACAAA), and r(AGCCUAACUCAGC)/d(GCTGAGTTAGGCT), within 68 duplexes examined here were non-two-state transitions. The two pentamers were too unstable to determine exactly the thermodynamics with the curve fitting procedure, and the two longer nucleotides might be due to non-two-state transitions frequently observed for longer oligonucleotides.

Nearest-Neighbor Model for RNA/DNA Hybrid Duplexes. The nearest-neighbor model in which the effect of nearest-neighbor base pairs is the most important for determining duplex stability is confirmed to be reasonable for most short DNA/DNA and RNA/RNA double helixes (Kierzek et al., 1986; Sugimoto et al., 1994). It should be confirmed whether the model can be applied to the RNA/DNA hybrids before obtaining the nearest-neighbor parameters. We examined energetic behaviors of six pairs of RNA/DNA hybrid duplexes with identical nearest neighbors (see Table 1). Each pair of the hybrid duplexes consists of identical nearest neighbors; for example, in the case of pair [1],

$$\text{r(CUUACGCU)/d(AGCGTAAG)} = \text{rCU/dAG} + \text{rUU/dAA} + \text{rUA/dTA} + \text{rAC/dGT} + \text{rCG/dCG} + \text{rGC/dGC} + \text{rCU/dAG} = \text{r(CUACGCUU)/d(AAGCGTAG)}$$

The nearest-neighbor hypothesis predicts that the pairs with identical nearest neighbors will have identical melting behaviors and identical thermodynamic parameters for duplex formation.

Figure 3 shows the T_m^{-1} vs ln(C_t/4) plots of pair [1] as typical plots, and the thermodynamic parameters for the duplex formation of pairs [1]−[6] obtained from eqs 1 and 2 are listed in Table 1; in eq 2,

$$\Delta G^\circ_{37} = \Delta H^\circ - (310.15 \times \Delta S^\circ) \quad (2)$$

Table 1: Thermodynamic Values of Duplex Formation of RNA/DNA Hybrids with Identical Nearest-Neighbor Sequences[a]

Pair #	Hybrid duplex	ΔH° / kcal mol^{-1}	ΔS° / cal mol^{-1}K^{-1}	ΔG°_{37} / kcal mol^{-1}	T_m[b] /°C
[1]	r(CUACGCUU)/d(AAGCGTAG)	-54.3	-153	-6.8	38.9
	r(CUUACGCU)/d(AGCGTAAG)	-52.3	-148	-6.4	36.2
[2]	r(ACCGCA)/d(TGCGGT)	-45.4	-126	-6.4	36.1
	r(GCACCG)/d(CGGTGC)	-49.7	-141	-6.2	34.8
[3]	r(CACGGC)/d(GCCGTG)	-48.9	-135	-6.9	39.5
	r(GGCACG)/d(CGTGCC)	-51.8	-144	-7.3	41.5
[4]	r(AAGCGUAG)/d(CTACGCTT)	-67.2	-192	-7.8	43.1
	r(AGCGUAAG)/d(CTTACGCT)	-60.1	-170	-7.3	41.1
[5]	r(AGUCCUGA)/d(TCAGGACT)	-54.7	-155	-6.7	37.9
	r(CUGAGUCC)/d(GGACTCAG)	-60.8	-171	-7.8	43.4
[6]	r(GAGCCGUG)/d(CACGGCTC)	-67.3	-187	-9.5	51.4
	r(GCCGUGAG)/d(CTCACGGC)	-71.4	-199	-9.7	51.4

[a] All experiments were conducted in a buffer containing 1 M NaCl/10 mM Na_2HPO_4/1 mM Na_2EDTA, pH 7.0. Estimated errors in ΔH°, ΔS°, ΔG_{37}°, and T_m are ±4%, ±4%, ±8%, and ±2%, respectively. [b] Melting temperatures are calculated at the total oligomer concentration of 100 μM.

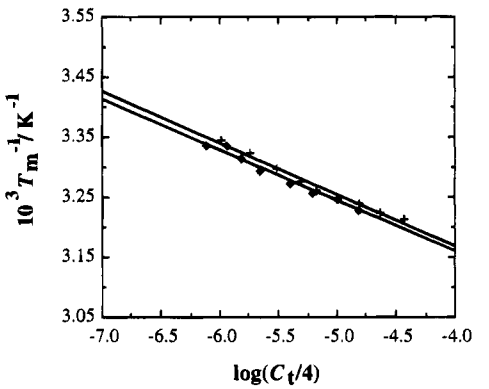

FIGURE 3: T_m^{-1} vs ln(C_t/4) plots of r(CUACGCUU)/d(AAGCGTAG) (♦) and r(CUUACGCU)/d(AGCGTAAG) (+). Measurements were done in 1 M NaCl−phosphate buffer at different oligomer concentrations.

where $\Delta G°_{37}$ is the change of free energy associated with hybrid duplex formation at 37.0 °C. In the pairs composed of identical nearest-neighbor sets, the melting curve traces at the same strand concentration (data not shown) were very similar, and both T_m^{-1} vs $\ln(C_t/4)$ plots for pair [1] in Figure 3 are almost identical. The values of $\Delta H°$, $\Delta S°$, $\Delta G°_{37}$, and T_m for pair [1] in Table 1 differ by only 3.8%, 3.3%, 6.1%, and 2.7 °C, respectively. For the other pairs in Table 1, the average differences in $\Delta H°$, $\Delta S°$, $\Delta G°_{37}$, and T_m are 7.7%, 8.2%, 6.5%, and 2.3 °C, respectively, about the same as expected from experimental errors. These results indicate that the nearest-neighbor model is valid for RNA/DNA hybrid duplexes as well as RNA/RNA and DNA/DNA duplexes.

Nearest-Neighbor Parameters for RNA/DNA Hybrid Duplexes. According to the nearest-neighbor model, formation of hybrid duplexes can be described by 16 nearest-neighbor parameters for helix propagation and 1 parameter for duplex initiation. To determine the nearest-neighbor parameters, thermodynamics for 68 different hybrid sequences including the duplexes with identical nearest neighbors described above was examined. The averaged thermodynamic parameters determined from the T_m^{-1} vs $\ln(C_t/4)$ plot and the curve fitting procedure are listed in Table 2. The melting temperatures at the strand concentration of 100 μM are also listed in the table. The optimized values for 16 nearest-neighbor sets and 1 initiation factor determined on the basis of the thermodynamic results of 64 hybrids with two-state transitions by using the nonlinear least-squares computer program are shown in Table 3. The $\Delta H°$, $\Delta S°$, $\Delta G°_{37}$, and T_m of 68 hybrids predicted with the parameters in Table 3 are also listed in Table 2.

DISCUSSION

Comparison of Hybrid Nearest-Neighbor Parameters with Those for DNA/DNA and RNA/RNA Helixes. In Table 3, $\Delta H°$ of RNA/DNA hybrid initiation is 1.9 kcal mol^{-1} rather than 0 kcal mol^{-1} as assumed for DNA/DNA and RNA/RNA parameters (Breslauer et al., 1986; Freier et al., 1986). This value is one of the parameters determined from the thermodynamic results in Table 2 and is assumed to be independent of oligonucleotides. Considering $\Delta G°_{37}$ of the initiation is 3.1 kcal mol^{-1}, it is suggested that the enthalpy contribution to initiation of at least hybrid formation is more important than the entropy contribution.

Generally, comparing $\Delta G°_{37}$ values of the hybrids with DNA/DNA (Breslauer et al., 1986) and RNA/RNA parameters (Freier et al., 1986), the RNA/RNA double helix is the most stable of the three kinds of helixes with the same nearest neighbors. Which is more stable between DNA/DNA and RNA/DNA hybrid duplexes seems to depend on its sequence: For example, dCG/dCG is more stable than rCG/dCG ($\Delta G°_{37}$ values are -3.3 and -1.7 kcal mol^{-1}, respectively), while rAC/dGT of -2.1 kcal mol^{-1} has larger stability than dAC/dGT of -1.1 kcal mol^{-1}.

The nearest-neighbor pairs of the hybrids with the most or least stable free energy are identical to the pairs of DNA/DNA and RNA/RNA duplexes. The nearest-neighbor sequences rGG/dCC and rGC/dGC have the largest absolute $\Delta G°_{37}$ values (-2.9 and -2.7 kcal mol^{-1}, respectively); such a tendency occurs also in the DNA/DNA and RNA/RNA duplexes (Breslauer et al., 1986; Freier et al., 1986). In contrast, rUU/dAA and rUA/dTA possess the smallest and the second smallest free energies in absolute values (-0.2 and -0.6 kcal mol^{-1}, respectively) in the hybrid nearest-neighbor pairs, which is also true for DNA/DNA and RNA/RNA duplexes. It suggests that in most cases hybrid formation does not stabilize or destabilize certain nearest-neighbor pairs in comparison with DNA/DNA and RNA/RNA double helixes.

But the case of rUU/dAA seems to be an exception. The $\Delta G°_{37}$ value of -0.2 kcal mol^{-1} is significantly smaller than those of dTT/dAA and rUU/rAA (-1.7 and -0.9 kcal mol^{-1}, respectively) and is also the smallest of all the hybrid values. The result is consistent with the experimental result previously reported that hybrid duplexes containing oligo(rU/dA) sequences are exceptionally unstable (Martin et al., 1980). The exclusive instability of dA_8/rU_8 should be primarily due to unstable rUU/dAA nearest-neighbor base pair.

Comparison of Measured and Predicted Thermodynamic Values for RNA/DNA Hybrid Formation. We calculated $\Delta G°_{37}$ values of 68 RNA/DNA hybrid duplexes with our hybrid parameters listed in Table 3. For example, the predicted free energy change of r(CUUACGCU)/d(AGCGTAAG) and r(CUACGCUU)/d(AAGCGTAG) with identical nearest neighbors described above can be calculated as follows:

$$\Delta G°_{37}(\text{predicted}) = \Delta G°_{37}(\text{rCU/dAG}) + \Delta G°_{37}(\text{rUU/dAA}) + \Delta G°_{37}(\text{rUA/dTA}) + \Delta G°_{37}(\text{rAC/dGT}) + \Delta G°_{37}(\text{rCG/dCG}) + \Delta G°_{37}(\text{rGC/dGC}) + \Delta G°_{37}(\text{rCU/dAG}) + \text{initiation factor} = -6.0 \text{ (kcal mol}^{-1}\text{)}$$

On the other hand, the measured values were -6.4 kcal mol^{-1} for r(CUUACGCU)/d(AGCGTAAG) and -6.8 kcal mol^{-1} for r(CUACGCUU)/d(AAGCGTAG) as shown in Table 2. The predicted and measured values are in good agreement with each other.

In comparison of the measured $\Delta G°_{37}$ values and the predicted ones as shown in Table 2, the average difference is only 5.4% for all the 64 sequences with the two-state transitions. The largest difference is 18% for r(GCGACAUU)/d(AAUGUCGC), of which the predicted and experimental values are -6.7 and -7.9 kcal mol^{-1}. For $\Delta H°$, $\Delta S°$, and T_m, the average differences are 6.8%, 7.6%, and 0.6%, respectively. These average errors are not so much larger than those of RNA duplex reported previously (Freier et al., 1986). Therefore, our parameters in Table 3 should be very useful to predict the thermodynamic stability of RNA/DNA hybrids.

Comparison with Other Parameters. To our knowledge, almost no nearest-neighbor parameters were determined previously for RNA/DNA hybrid duplex formation except for Yager and von Hippel's parameters (Yager & von Hippel, 1991). Unfortunately, in obtaining their parameters, many hypotheses had to be used because there were not enough experimental data at that time to determine exactly hybrid parameters. For example, the values for some nearest-neighbor sequences had to be calculated as an average of DNA/DNA parameters (Breslauer et al., 1986) and RNA/RNA parameters (Freier et al., 1986). As several nearest-neighbor pairs had to be regarded as possessing the same

Table 2: Measured and Predicted Thermodynamic Values for Hybrid Formation in 1 M NaCl Phosphate Buffer[a]

RNA sequence[b]	$\Delta H°$ (kcal mol^{-1})	$\Delta S°$ (cal mol^{-1} K^{-1})	$\Delta G°_{37}$ (kcal mol^{-1})	T_m[c] (°C)
AGCCG	−41.6 (−40.8)[d]	−116 (−115)	−5.7 (−5.2)	30.8 (27.2)
CGGCU	−45.8 (−42.2)	−132 (−120)	−4.9 (−5.1)	26.1 (26.7)
GGUGG	−46.0 (−41.9)	−132 (−118)	−5.2 (−5.4)	28.0 (28.8)
ACCGCA	−45.4 (−46.6)	−126 (−130)	−6.4 (−6.4)	36.1 (36.0)
CAAUCG	−46.7 (−48.1)	−140 (−146)	−3.3 (−2.9)	16.9 (15.1)
CACGGC	−48.9 (−50.1)	−135 (−138)	−6.9 (−7.2)	39.5 (41.0)
CGAUUG	−49.3 (−50.1)	−151 (−153)	−2.6 (−2.6)	14.1 (14.4)
CGGUGC	−48.9 (−53.4)	−135 (−150)	−7.0 (−6.9)	40.1 (39.0)
CGUGCC	−49.3 (−49.9)	−139 (−141)	−6.3 (−6.1)	35.3 (34.2)
GCACCG	−49.7 (−46.6)	−141 (−130)	−6.2 (−6.4)	34.8 (36.0)
GGCACG	−51.8 (−50.1)	−144 (−138)	−7.3 (−7.2)	41.5 (41.0)
AAUACCG	−54.1 (−53.5)	−160 (−156)	−4.7 (−5.3)	26.6 (29.9)
ACGUAUG	−58.3 (−54.6)	−172 (−160)	−5.0 (−4.9)	29.6 (27.8)
AGCUUCA	−55.6 (−51.3)	−164 (−150)	−4.7 (−4.9)	26.2 (27.5)
CACGGCU	−53.9 (−57.1)	−147 (−158)	−8.5 (−8.1)	48.6 (45.6)
CAUACGU	−53.2 (−53.2)	−158 (−158)	−4.3 (−4.2)	24.5 (23.8)
GGACUUA	−43.8 (−48.6)	−125 (−141)	−4.9 (−4.9)	25.9 (26.9)
UAAGUCC	−46.2 (−48.5)	−132 (−140)	−5.4 (−5.0)	29.4 (27.6)
UGAAGCU	−43.0 (−45.9)	−118 (−128)	−6.4 (−6.2)	36.5 (34.8)
AAAAAAAA	−54.0 (−52.7)	−162 (−157)	−3.8 (−3.9)	22.1 (22.5)
AAGCGUAG	−67.2 (−64.0)	−192 (−182)	−7.8 (−7.6)	43.1 (42.3)
AAUCCAGU	−55.9 (−58.0)	−161 (−167)	−6.1 (−6.2)	34.5 (35.3)
AAUGUCGC	−64.9 (−65.3)	−186 (−187)	−7.2 (−7.4)	39.9 (41.0)
ACCUAGUC	−56.0 (−53.6)	−159 (−150)	−6.9 (−7.0)	39.2 (39.7)
ACGACCUC	−55.0 (−56.6)	−150 (−155)	−8.6 (−8.6)	48.9 (48.5)
ACUGGAUU	−57.8 (−59.5)	−163 (−170)	−7.2 (−6.8)	40.9 (38.3)
AGCGUAAG	−60.1 (−64.0)	−170 (−182)	−7.3 (−7.6)	41.1 (42.3)
AGUCCUGA	−54.7 (−55.8)	−155 (−157)	−6.7 (−7.2)	37.9 (40.8)
CAACAGCA	−52.7 (−55.9)	−145 (−157)	−7.8 (−7.2)	44.8 (40.8)
CACGGCUC	−71.6 (−65.7)	−200 (−181)	−9.6 (−9.6)	50.5 (52.0)
CGCUGUAA	−60.4 (−63.2)	−172 (−183)	−7.2 (−6.5)	40.2 (36.7)
CUACGCUU	−54.3 (−61.6)	−153 (−179)	−6.8 (−6.0)	38.9 (34.2)
CUAGUGGA	−63.4 (−58.5)	−178 (−166)	−8.3 (−7.1)	45.1 (40.1)
CUCACGGC	−70.3 (−65.7)	−196 (−181)	−9.6 (−9.6)	51.0 (52.0)
CUGAGUCC	−60.8 (−55.8)	−171 (−157)	−7.8 (−7.2)	43.4 (40.8)
CUUACGCU	−52.3 (−61.6)	−148 (−179)	−6.4 (−6.0)	36.2 (34.2)
GACUAGGU	−57.0 (−54.0)	−158 (−150)	−8.1 (−7.6)	45.9 (43.3)
GAGCCGUG	−67.3 (−64.5)	−187 (−178)	−9.5 (−9.2)	51.4 (50.4)
GAGGUCGU	−71.9 (−66.0)	−202 (−186)	−9.2 (−8.3)	48.9 (45.6)
GCCAGUUA	−62.9 (−60.6)	−180 (−175)	−7.2 (−6.3)	40.0 (35.9)
GCCGUGAG	−71.4 (−64.5)	−199 (−178)	−9.7 (−9.2)	51.4 (50.4)
GCGACAUU	−60.6 (−62.6)	−170 (−180)	−7.9 (−6.7)	43.9 (37.7)
UAACUGGC	−62.6 (−57.8)	−174 (−158)	−8.6 (−8.7)	47.7 (48.9)
UCCACUAG	−64.1 (−54.8)	−184 (−155)	−6.9 (−6.8)	38.6 (38.5)
UGCUGUUG	−52.0 (−63.6)	−146 (−184)	−6.7 (−6.6)	38.3 (37.2)
UGUUCGAC	−66.2 (−64.1)	−190 (−186)	−7.4 (−6.4)	41.3 (36.3)
UUACAGCG	−58.4 (−65.7)	−166 (−190)	−7.0 (−6.9)	39.5 (38.7)
UUGGCACC	−56.2 (−65.0)	−153 (−179)	−8.7 (−9.4)	49.8 (51.3)
AUAACUGGC	−60.7 (−66.1)	−168 (−182)	−8.7 (−9.6)	48.7 (51.9)
AUCUAUCCG	−59.9 (−72.3)	−171 (−210)	−6.8 (−7.0)	38.4 (38.8)
CAACAGCAA	−63.3 (−63.7)	−177 (−179)	−8.7 (−8.2)	47.8 (45.4)
CAACAGCAU	−71.0 (−64.2)	−200 (−181)	−9.0 (−8.1)	48.1 (44.7)
CGCUGUUAC	−71.5 (−72.8)	−205 (−210)	−8.2 (−7.8)	44.2 (42.3)
CGCUGUUAG	−67.7 (−76.0)	−193 (−221)	−8.0 (−7.5)	44.0 (41.0)
CUAACAGCG	−70.8 (−69.0)	−199 (−195)	−9.0 (−8.6)	48.1 (46.5)
GCCAGUUAA	−63.1 (−68.4)	−179 (−197)	−7.7 (−7.3)	42.7 (40.7)
GUAACAGCG	−77.5 (−69.8)	−221 (−197)	−9.1 (−8.8)	47.8 (47.4)
UUAACUGGC	−67.3 (−69.3)	−189 (−195)	−8.9 (−8.9)	48.3 (47.9)
ACGUAUUAUGC	−95.4 (−90.2)	−279 (−261)	−9.1 (−9.3)	45.6 (46.6)
GCAUAAUACGU	−97.3 (−85.1)	−282 (−244)	−10.0 (−9.4)	48.4 (47.7)
AAUGGAUUACAA	−90.7 (−93.2)	−260 (−267)	−10.2 (−10.3)	50.2 (50.1)
AUUGGAUACAAA	−93.6 (−93.2)	−267 (−267)	−10.8 (−10.3)	51.9 (50.1)
GUCAGGAAUCUG	−79.8 (−93.0)	−220 (−260)	−11.4 (−12.3)	57.4 (57.5)
UUGUAAUCCAUU	−76.9 (−98.4)	−221 (−292)	−8.5 (−7.9)	45.4 (41.4)
		Non-Two-State Transitions		
CGUGC	−48.3 (−40.6)	−149 (−118)	−2.3 (−4.0)	14.2 (18.6)
GCACG	−46.8 (−37.3)	−134 (−107)	−5.0 (−4.3)	27.1 (19.3)
UUUGUAUCCAAU	−84.9 (−98.4)	−246 (−292)	−8.8 (−7.9)	45.6 (41.4)
AGCCUAACUCAGC	−85.2 (−94.7)	−236 (−254)	−12.1 (−15.9)	59.3 (71.0)

[a] All experiments were conducted in a buffer containing 1 M NaCl/10 mM Na_2HPO_4/1 mM Na_2EDTA, pH 7.0. Estimated errors in $\Delta H°$, $\Delta S°$, $\Delta G°_{37}$, and T_m are ±4%, ±4%, ±3%, and ±2%, respectively. [b] A hybrid duplex consists of the denoted RNA strand and its complementary DNA strand. [c] Melting temperatures are calculated at the total oligomer strand concentration of 100 μM. [d] The values in parentheses are predicted with the parameters in Table 3. These values agree with the measured ones within average errors of 6.8% for $\Delta H°$, 7.6% for $\Delta S°$, 5.4% for $\Delta G°_{37}$, and 0.6% for T_m.

Table 3: Thermodynamic Parameters for Hybrid Duplex Initiation and Propagation in 1 M NaCl Buffer[a]

Sequence	$\Delta H°$ / kcal mol^{-1}	$\Delta S°$ / cal mol^{-1} K^{-1}	$\Delta G°_{37}$ / kcal mol^{-1}
rAA dTT	-7.8	-21.9	-1.0
rAC dTG	-5.9	-12.3	-2.1
rAG dTC	-9.1	-23.5	-1.8
rAU dTA	-8.3	-23.9	-0.9
rCA dGT	-9.0	-26.1	-0.9
rCC dGG	-9.3	-23.2	-2.1
rCG dGC	-16.3	-47.1	-1.7
rCU dGA	-7.0	-19.7	-0.9
rGA dCT	-5.5	-13.5	-1.3
rGC dCG	-8.0	-17.1	-2.7
rGG dCC	-12.8	-31.9	-2.9
rGU dCA	-7.8	-21.6	-1.1
rUA dAT	-7.8	-23.2	-0.6
rUC dAG	-8.6	-22.9	-1.5
rUG dAC	-10.4	-28.4	-1.6
rUU dAA	-11.5	-36.4	-0.2
initiation	1.9	-3.9	3.1

[a] Estimated errors in $\Delta H°$, $\Delta S°$, and $\Delta G_{37}°$ are ± 0.3 kcal mol^{-1}, ± 1.3 cal mol^{-1} K^{-1}, and ± 0.1 kcal mol^{-1}, respectively.

free energy change, each thermodynamic value did not always reflect one nearest-neighbor sequence. Helix initiation factor also had to be estimated from melting studies on a homologous series of DNA/DNA duplexes (Gralla & Crothers, 1973). Accordingly, the nearest-neighbor parameters obtained with these hypotheses cannot estimate the stability of RNA/DNA hybrid duplexes with high accuracy.

Comparing our parameters with Yager and von Hippel's parameters, helix initiation factors are similar; our value is 3.1 kcal mol^{-1} while his value is 3.0 kcal mol^{-1}. But there are very large differences of free energies for many nearest-neighbor sequences. For example, rUA/dTA has $\Delta G°_{37}$ of -0.6 kcal mol^{-1} for our parameters, but -1.3 kcal mol^{-1} for Yager and von Hippel's assumptions. The average difference between the measured values and predicted values from their parameters is 27%, and the largest difference is 48%. These differences are much larger than those from our parameters (5.4% and 18%, respectively). Thus, our parameters should give improved predictions for the stability of RNA/DNA hybrids.

SUPPORTING INFORMATION AVAILABLE

Two tables listing thermodynamic parameters obtained with the T_m^{-1} vs $\ln(C_t/4)$ plot and the curve fitting procedure (6 pages). Ordering information is given on any current masthead page.

REFERENCES

Bevington, P. R. (1969) in *Data Reduction and Error Analysis for the Physical Sciences*, McGraw-Hill, New York, NY.

Breslauer, K. J., Frank, R., Blöcker, H., & Marky, L. A. (1986) *Proc. Natl. Acad. Sci. U.S.A. 83*, 3746–3750.

Connell, G. J., & Yarus, M. (1994) *Science 264*, 1137–1141.

Freier, S. M., Kierzek, R., Jaeger, J. A., Sugimoto, N., Caruthers, M. H., Neilson, T., & Turner, D. H. (1986) *Proc. Natl. Acad. Sci. U.S.A. 83*, 9373–9377.

Gralla, J., & Crothers, D. M. (1973) *J. Mol. Biol. 78*, 301–309.

Hall, K. B., & McLaughlin, L. W. (1991) *Biochemistry 30*, 10606–10613.

Ivanov, V. I., Minchenkova, L. E., Schyolkina, A. K., & Poletayev, A. I. (1973) *Biopolymers 12*, 89–100.

Kierzek, R., Caruthers, M. H., Longfellow, C. E., Swinton, D., Turner, D. H., & Freier, S. M. (1986) *Biochemistry 25*, 7840–7846.

LeCuyer, K. A., & Crothers, D. M. (1993) *Biochemistry 32*, 5301–5311.

Longfellow, C. E., Kierzek, R., & Turner, D. H. (1990) *Biochemistry 29*, 278–285.

Martin, F. H., & Tinoco, I., Jr. (1980) *Nucleic Acids Res. 8*, 2295–2299.

McCalla, T. R. (1967) in *Introduction to Numerical Methods and FORTRAN Programming*, John Wiley & Sons, New York, NY.

Ogawa, T., & Okazaki, T. (1980) *Ann. Rev. Biochem. 49*, 421–457.

Peritz, A. E., Kierzek, R., Sugimoto, N., & Turner, D. H. (1991) *Biochemistry 30*, 6428–6436.

Petersheim, M., & Turner, D. H. (1983) *Biochemistry 22*, 256–263.

Ratmeyer, L., Vinayak, R., Zhong, Y. Y., Zon, G., & Wilson, D. (1994) *Biochemistry 33*, 5298–5304.

Richards, E. G. (1975) in *Handbook of Biochemistry and Molecular Biology: Nucleic Acids* (Fasman, G. D., Ed.) 3rd ed., Vol. 1, p 597, CRC Press, Cleveland, OH.

Shimayama, T., Nishikawa, F., Nishikawa, S., & Taira, K. (1993) *Nucleic Acids Res. 21*, 2605–2611.

Stein, C. A., & Cheng, Y.-C. (1993) *Science 261*, 1004–1012.

Sugimoto, N., & Sasaki, M. (1991) *Chem. Lett.*, 345–348.

Sugimoto, N., Kierzek, R., Freier, S. M., & Turner, D. H. (1986) *Biochemistry 25*, 5755–5759.

Sugimoto, N., Kierzek, R., & Turner, D. H. (1987a) *Biochemistry 26*, 4554–4558.

Sugimoto, N., Kierzek, R., & Turner, D. H. (1987b) *Biochemistry 26*, 4559–4562.

Sugimoto, N., Tanaka, A., Shintani, Y., & Sasaki, M. (1991) *Chem. Lett.*, 9–12.

Sugimoto, N., Sasaki, M., & Tanaka, A. (1993) *Supramol. Chem. 2*, 99–102.

Sugimoto, N., Honda, K., & Sasaki, M. (1994) *Nucleosides Nucleotides 13*, 1311–1317.

Turner, D. H., Sugimoto, N., & Freier, S. M. (1990) in *Landolt-Børnstein Nucleic Acids* (Saenger, W. R., Ed.) Vol. 1c, Chapter 3.6, Berlin, Germany.

Varmus, H. E. (1982) *Science 216*, 812–820.

Yager, T. D., & von Hippel, P. H. (1991) *Biochemistry 30*, 1097–1118.

BI950894D